

Signal quality quantification and waveform reconstruction of arterial blood pressure recordings

A. Fanelli, *Member, IEEE*, and T. Heldt, *Senior Member, IEEE*

Abstract— Arterial blood pressure (ABP) is an important vital sign of the cardiovascular system. As with other physiological signals, its measurement can be corrupted by different sources of noise, interference, and artifact. Here, we present an algorithm for the quantification of signal quality and for the reconstruction of the ABP waveform in noise-corrupted segments of the measurement. The algorithm quantifies the quality of the ABP signal on a beat-by-beat basis by computing the normalized mean of successive differences of the ABP amplitude over each beat. In segments of poor signal quality, the ABP wavelets are then reconstructed on the basis of the expected cycle duration and envelope information derived from neighboring ABP wavelet segments. The algorithm was tested on two datasets of ABP waveform signals containing both invasive radial artery ABP and noninvasive ABP waveforms. Our results show that the approach is efficient in identifying the noisy segments (accuracy, sensitivity and specificity over 95%) and reliable in reconstructing beats that were artificially corrupted.

I. INTRODUCTION

The arterial pulse is a cardinal vital sign of the cardiovascular system [1,2], and several approaches are available for arterial blood pressure (ABP) measurement [3]. Invasive and noninvasive techniques are available for continuous measurement of the ABP waveform [4]. The gold standard measurement in critical care environments is by invasive radial artery catheterization. In experimental settings, noninvasive methods are also available for ABP monitoring [5].

In both settings, the ABP measurement is often subject to noise and artifact. Moreover, ABP measured through noninvasive sensors can be affected by recurrent signal calibration phases that interrupt the physiologic waveform. Such transient signal loss or corruption is normally not a significant problem in clinical practice. However, several approaches to advanced ABP waveform analysis, such as cardiac output [6] or intracranial pressure estimation [7], rely on a high-quality ABP signal to be fed into the estimation algorithm. If the quality of the acquired ABP signal is insufficient, the quality of the resultant estimates cannot be trusted. Likewise, if the acquired ABP signal suffers from frequent, short intermittent signal loss (automated recalibrations) a significant amount of the acquired signal might need to be discarded. The assessment of signal quality

and possible imputation of realistic waveform signals over short periods of data loss therefore becomes an important preprocessing step.

This study presents an algorithm that detects the regions of the ABP signal that are affected by artifacts. This is accomplished through an index that quantifies signal quality beat-by-beat. The algorithm subsequently reconstructs the ABP wavelets during the noisy segments through an averaging approach. We tested both the reliability in quality quantification and the fidelity in signal reconstruction. Our results show that the approach is effective in processing ABP signal and reconstructing noisy regions with new synthetic beats.

II. METHODS

The algorithm is characterized by four steps: signal preprocessing, beat-onset correction, signal-quality computation, and ABP signal reconstruction.

A. Signal preprocessing

The first step of the algorithm consists in ABP signal preprocessing. We apply a 16Hz low-pass filter to remove unphysiologic high-frequency noise. For this purpose, data records were up-sampled to 120Hz from their native sampling frequency of 40 to 70Hz using linear interpolation. ABP beat onsets were then detected by using the algorithm developed by Zong *et al.* [8]. The algorithm marks the onset of each individual blood pressure wavelet using a curve-length transform.

B. Beat Onset Correction

Correct onset detection represents the first and most important preprocessing step of the entire approach. The success in signal-quality evaluation and ABP wavelet reconstruction relies on accurate beat-onset detection. Depending on the quality of the ABP signal, the beat-onset detection algorithm in [8] can produce a significant number of false-positive detections that negatively affect the subsequent steps of our approach. For this reason, we introduced an automated correction of the detected onsets. The correction works by assuming that the i -th detected onset is correct, and by looking for the most reasonable $(i+1)$ -th onset, among the subsequent ten detections provided by Zong's algorithm. This is accomplished by computing the average inter-beat interval (Δt_{mean}) of the last 5 detections that have been flagged as correct. This value is used as reference to identify subsequent correct detections. The onset among the 10 future detections that is closest in terms of temporal distance to Δt_{mean} , is selected as the correct $(i+1)$ -th onset.

*Research supported by Maxim Integrated through the MIT Medical Electronic Device Realization Center.

A. Fanelli and T. Heldt are with the Integrative Neuromonitoring and Critical Care Informatics Group, Institute for Medical Engineering and Science, Massachusetts Institute of Technology, Cambridge, MA (corresponding author e-mail: fanelli@mit.edu).

C. Quality computation

Computation of waveform quality is crucial to identify which signal segments are corrupted and require reconstruction. We defined a quality parameter that quantifies signal quality beat-by-beat. We begin by computing the mean q_i of successive differences of the ABP amplitude over each beat i :

$$q_i = \text{mean}_j \|ABP(j) - ABP(j+1)\|,$$

$$j = n(i), n(i)+1, n(i)+2, \dots, n(i+1)-1$$

Here, n denotes the series of beat onsets and $[n(i), n(i+1)]$ spans all samples of the i -th beat. The parameter q_i will be very large in regions of high noise, or essentially zero in regions of an unphysiologically flat waveform (recalibration). The parameter q_i is then normalized to the signal history of this mean first-difference.

$$q = \frac{\|q_i - \bar{q}_i\|}{q_i}, \text{ where}$$

$$\bar{q}_i = \frac{1}{20}(q_{i-1} + q_{i-2} + q_{i-3} + \dots + q_{i-21}).$$

An empirical threshold of 0.3 was set to flag bad signal segments. Each beat onset is thus assigned a flag-value of 1 if the subsequent ABP wavelet is of poor quality, or a value of 0 if the following ABP wavelet is of good quality.

D. Signal reconstruction

Signal reconstruction is accomplished on data windows of 60 beats, overlapped of 50%. Inside each 60-beat window, all regions flagged as noisy go through the signal reconstruction step. In order to avoid border effects, the beat immediately before and the one immediately following a region of poor signal quality are also reconstructed. The reconstruction phase can be divided into 3 steps:

Step 1: Definition of beats duration. The first step of the reconstruction identifies the average number of beats that

The algorithm computes the average duration $\overline{t_{beat}}$ of all good-quality beats over a running 60-second window. The duration of the current noisy segment Δt_{noisy} is divided by $\overline{t_{beat}}$. This operation returns the approximate number N of beats that need to be reconstructed inside the current noisy signal segment. Then Δt_{noisy} is divided by N in order to obtain the duration of each beat \hat{t}_{beat} . Each noisy segment will be reconstructed with beats of the same duration.

Step 2: Definition of beat shape. Inside each noisy segment, the shape of each reconstructed ABP wavelet is obtained by computing the time average of all the good-quality ABP wavelets within the 60-second window. Before computing the time average, each good-quality beat is compressed or dilated in time to the average beat duration \hat{t}_{beat} . In this way, the average ABP wavelet also has the duration \hat{t}_{beat} .

Step 3: Definition of beat amplitude and offset. To determine the ABP wavelet amplitude two interpolating functions are computed. The first function is the interpolator of the diastolic ABP values over the 60-beat window, excluding the onsets belonging to the noisy data segments in the window. The curve is obtained through a piecewise cubic Hermite interpolation [9]. The second curve is the interpolator of the blood pressure systolic peaks of the good beats over the same 60-beat window. The peaks are identified as the maximum of the arterial blood pressure signal in a window of 200ms starting from each onset. For the systolic peaks, $SAP(t)$, a Fourier series interpolator was used

$$SAP(t) = a_0 + a_1 \cos(\omega t) + b_1 \sin(\omega t) + \dots + a_4 \cos(4\omega t) + b_4 \sin(4\omega t)$$

where the algorithm estimates the amplitude coefficients a_i and b_i , as well as the frequency ω . To reconstruct each

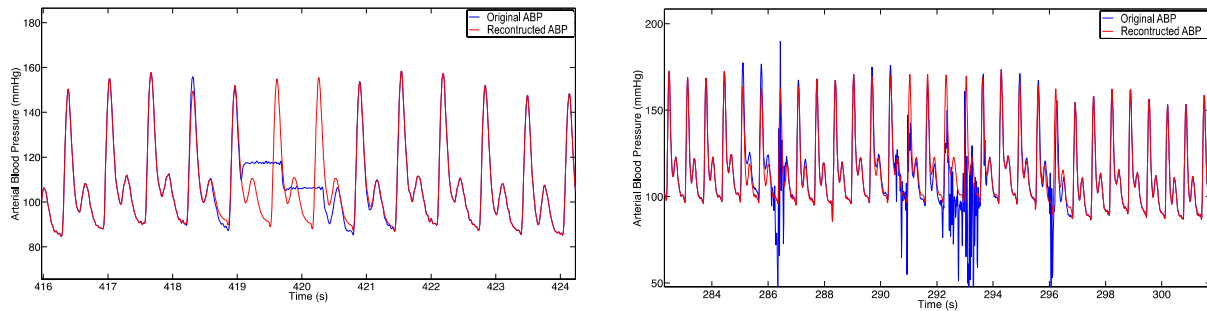


Fig. 1 Left: Example of ABP reconstruction in a Finapres ABP waveform affected by intermittent recalibration. Right: Example of ABP reconstruction of a radial artery ABP waveform affected by high-frequency noise. In both plots, the blue signal is the original ABP waveform and the red signal is the reconstructed waveform.

the algorithm should reconstruct in each noisy segment.

ABP wavelet in the noisy data segment, the amplitude of

each beat shape is stretched such that the reconstructed beat's systolic and diastolic values coincide with the envelope functions.

III. RESULTS

The algorithm was tested on two different datasets of ABP signals in which invasive and noninvasive continuous ABP signals were available.

The first dataset is composed of 48 archived records from 11 patients, recorded at Addenbrooke's Hospital in Cambridge, UK. Each file includes simultaneous waveforms of ABP from radial artery catheterization, cerebral blood flow velocity (CBFV) from transcranial Doppler (TCD) ultrasonography of the middle cerebral artery (MCA), intracranial pressure (ICP) from an indwelling parenchymal probe, and ABP from a Finapres sensor (Datex-Ohmeda Finapres). The algorithm was tested on both Finapres and radial ABP. Data sampling frequency is 50Hz. Record lengths range from 5 to 60 minutes.

The second dataset was also recorded at Addenbrooke's Hospital, Cambridge, UK and contains 45 records from 37 patients. Each patient record consists of invasive ICP waveform, continuous waveforms of ABP from radial-artery catheterization and CBFV from TCD ultrasonography of the MCA. The record lengths range from 10 to 240 min. Sampling frequency ranges from 40 to 70 Hz.

Figure 1 shows how the algorithm reconstructs two noisy segments of two ABP waveforms. The original (noisy) ABP waveforms are plotted in blue, and the reconstructed waveforms are shown in red superimposed.

In the left panel of Figure 1, the original ABP waveform is affected by a recalibration event. Such recalibration events intermittently affect ABP waveforms recorded by a Finapres sensor. The sensor goes through regular automatic calibration, which causes a square-wave artifact in the recorded signal. These events can vary in duration and frequency, but tend to last between three to six beats and occur at least once a minute.

The quality parameter correctly identifies the affected region, and the reconstruction allows filling the waveform gap with plausible synthetic beats. By design, the shape of the synthetic beats resembles the shape of the beats surrounding the noisy region. Moreover, the sinusoidal

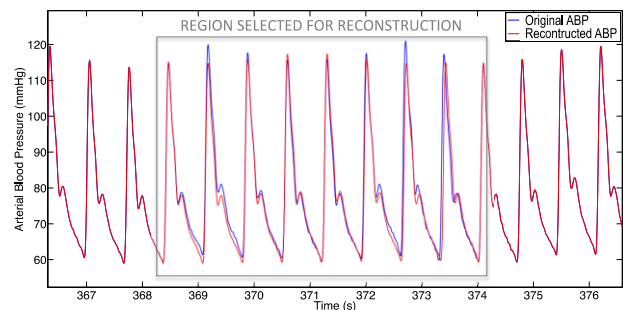


Fig. 2 Example of beat reconstruction. The 8-beats window was flagged as noisy in order to have a direct comparison between original and reconstructed ABP and to have an indication of fidelity in beat reconstruction.

pattern of the systolic peaks is preserved thanks to the sinusoidal interpolator. As described in the previous section, the beat immediately before and the beat immediately following the calibration phase are also reconstructed, in order to avoid undesirable edge effects.

The right panel in Figure 1 shows an example of ABP reconstruction in a waveform segment affected by high-frequency noise. The quality parameter correctly identifies the noisy region, and the reconstruction is efficient in filling the noisy segments with clean, plausible beats.

A. Validation

In order to validate the performance of the entire approach, we proceeded by evaluating the following two tasks: (i) ability to detect noisy segments and (ii) fidelity in beats reconstruction.

To validate the performance of the quality parameter in identifying noisy segments, we compared the automatic quality annotations of the algorithm to the manual annotations performed by two operators. Two expert operators inspected 14 ABP waveform records in the first data set and 4 ABP waveform records in the second data set. These sets were randomly selected from among the available data records. Noisy beats were manually annotated using the WFDB software package available on PhysioNet.org [10]. We computed sensitivity, specificity and accuracy by determining the true positives (*TP*), the false positives (*FP*), the true negatives (*TN*), and the false negatives (*FN*). We

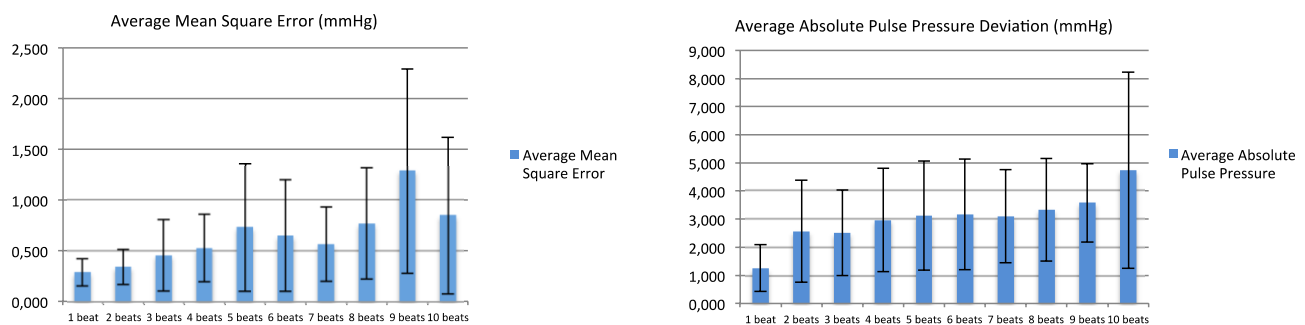


Fig. 3 The histograms show how the average mean square error changes as we increase the length of the window that is reconstructed (left) and how the average absolute pulse pressure deviation increases as we increase the length of the window.

obtained an overall accuracy $(TP+TN)/(TP+TN+FP+FN)$ of 99%, a sensitivity $TP/(TP+FN)$ of 95%, and specificity $TN/(TN+FP)$ of 99%. In order to compare the difference between algorithm performance and human performance to the normal inter-operator variability, we also computed sensitivity, specificity and accuracy of one operator with respect to the other. For the inter-operator comparison, we obtain an accuracy of 99%, a sensitivity of 99% and a specificity of 99%. The performance of the algorithm is therefore comparable with human performance in identifying noisy beats.

To quantify the fidelity of the wavelet reconstruction, we proceeded by reconstructing ABP segments of good signal quality, pretending they have been flagged as noisy by the algorithm. In this way it is possible to directly compare the result of the reconstruction to the underlying real ABP signal. The analysis was performed on 10 recordings belonging to the second data set. For each record, 20 non-overlapping windows were selected, of a length ranging from 1 to 10 beats. The starting beat and the number of beats in each window were selected randomly, thus assuring that no beats in each window were flagged as noisy. Figure 2 shows an example of the wavelet reconstruction, where the blue plot represents the original ABP while the red plot is the reconstructed ABP.

To quantify the reconstruction accuracy, we computed the mean-square-error between the reconstructed ABP wavelets and the original ones, for each of the 20 windows in each record. The average mean-square-error was computed across all windows of all the records.

Figure 3 shows how the average mean square error increases as we increase the length of the reconstruction window. Even for 10-beat windows the average mean square error remains smaller than 1 mmHg. This confirms high fidelity in the shape of the reconstructed beats.

In order to evaluate how precisely systolic and diastolic pressure are estimated, we also computed the average absolute pulse pressure difference between original and reconstructed windows. Its value increases with the window length, but remains below 5 mmHg on average for a 10-beat reconstruction.

IV. DISCUSSION AND CONCLUSIONS

In this paper, a new algorithm for the detection and reconstruction of noisy segments in ABP signals is presented. The algorithm was tested on two different datasets containing both invasive and Finapres ABP signals. The algorithm correctly identified noisy waveform segments and reliably reconstructed the ABP wavelets corrupted by noise. The approach that is presented here does not require any prior training. The reconstruction is accomplished by using the clean beats of a 60-second data window.

This algorithm might have many applications: the ABP signal can be affected by many noise sources. Mainly in the case of Finapres data, the frequent recalibrations that are performed by the sensor drastically reduce the amount of data that can be used for analysis or further processing.

The algorithm described in this paper has some limitations. First of all, the temporal duration of all the beats that are reconstructed inside a noisy segment is the same. Second, within the same window, the same template is used to reconstruct all noisy beats. In order to overcome these limitations, we are currently working on a second version of the algorithm that employs a second physiological signal that was synchronously recorded along with the ABP signal (e.g., ECG, PPG, or cerebral blood flow velocity) to precisely identify the temporal position of each beat onset and to have more information for the reconstruction of the beat shape.

Even if the algorithm was tested only on arterial blood pressure data (and cerebral blood flow velocity data, not shown here), we believe that its structure is perfectly scalable and adaptable to other physiological waveforms, and can be used any time a quasi-periodic signal requires reconstruction. Finally, the simplicity of the algorithm makes its implementation on a microprocessor platform for wearable technology eminently feasible.

ACKNOWLEDGMENTS

The data used in this study were kindly provided by Prof. Marek Czosnyka of Addenbrooke's Hospital, University of Cambridge, Cambridge, UK.

REFERENCES

- [1] M.F. O'Rourke, R.P. Kelly, A.P. Aviola. *The arterial pulse*. Lea & Febiger. Malvern, PA, 1992.
- [2] M.F. O'Rourke and D.E. Gallagher, "Pulse wave analysis." *Journal of Hypertension*, vol. 14, n. 5, pp. S147-57, 1996.
- [3] D. Perloff, C. Grim, J. Flack, E.D. Frohlich, M. Hill, M. McDonald, and B.Z. Morgenstern. "Human blood pressure determination by sphygmomanometry." *Circulation*, vol. 88, n. 5, pp. 2460-2470, 1993.
- [4] H.W. Shirer. "Blood pressure measuring methods." *IRE Transactions on Bio-Medical Electronics*, vol. 9, n. 2, pp. 116-125, 1962.
- [5] K.H. Wesseling, "Finger arterial pressure measurement with Finapres." *Zeitschrift für Kardiologie*, vol. 85, pp. 38-44, 1995.
- [6] K.H. Wesseling, J.R. Jansen, J.J. Settles, J.J. Schreuder. "Computation of aortic flow from pressure in humans using a nonlinear, three-element Windkessel model." *Journal of Applied Physiology* vol. 74, nn. 5, pp. 2566-2573, 1985.
- [7] F.M. Kashif, G.C. Verghese, M. Czosnyka, V. Novak, T. Heldt, "Model-based noninvasive estimation of intracranial pressure from cerebral blood flow velocity and arterial blood pressure." *Science Translational Medicine*, vol. 4, nn. 129, pp. 129ra44, 2012.
- [8] W. Zon, T. Heldt, G.B. Moody, R.G. Mark, "An open-source algorithm to detect the onset of arterial blood pressure pulses." *Computers in Cardiology*, vol. 30, pp. 259-262, 2003.
- [9] F.N. Fritsch and R.E. Carlson, "Monotone Piecewise Cubic Interpolation." *SIAM J. Numerical Analysis*, vol. 17, pp. 238-246, 1980.
- [10] G.B. Moody, R.G. Mark, and A.L. Goldberger. "PhysioNet: a web-based resource for the study of physiologic signals." *IEEE Eng in Med and Biol*, vol. 20, n. 3, pp. 70-75, 2001.